Polarized synchrotron X-ray emission from supernova shells. XIPE perspective.

A.M. Bykov, Y.A. Uvarov
Ioffe Institute, St.Petersburg, Russia

Plan

1. SNR as a source of nonthermal emission.
2. Electron distribution function calculation near SNR shock front.
3. Simulation of the turbulent magnetic field.
   - isotropic turbulence
   - anisotropic axisymmetric turbulence
4. Synchrotron radiation and simulation of SNR X-ray intensity and polarization maps.
5. New generation of X-ray polarimeters and XIPE.
6. Simulation of SNR X-ray intensity and polarization maps with XIPE angular resolution.

Polarized synchrotron X-ray emission from supernova shells. XIPE perspective.

A.M. Bykov, Y.A. Uvarov

SN 1006

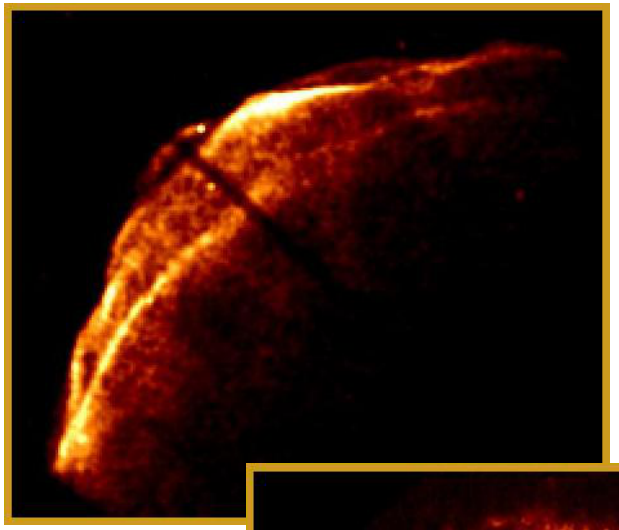

Cas A

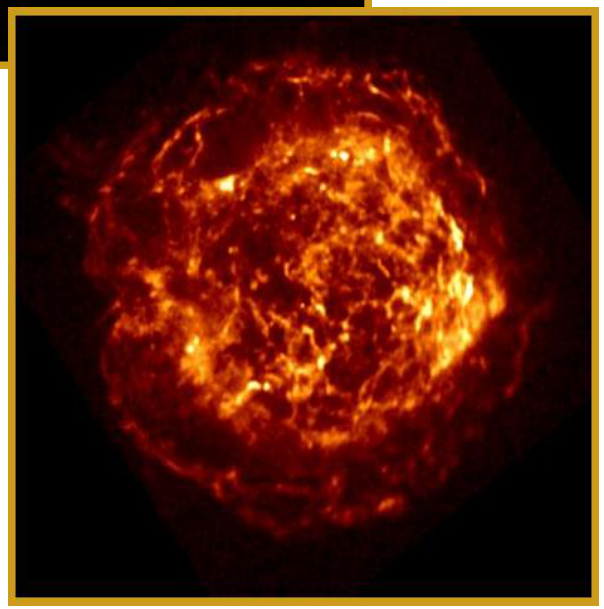

RX 1713.7-3946

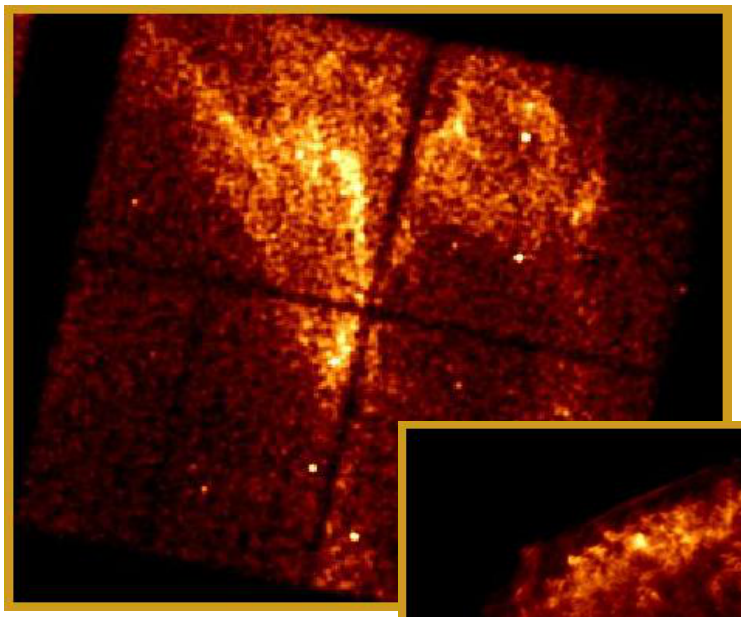

Tycho

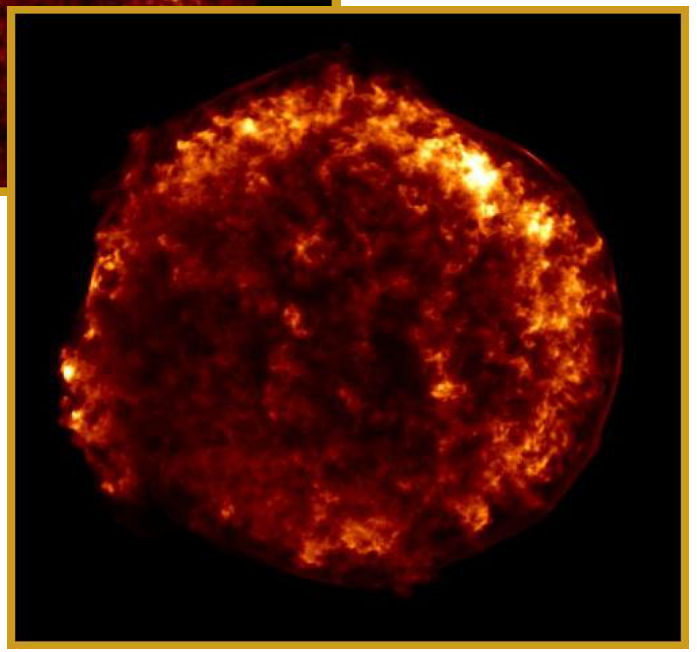

Fermi acceleration at shock - I.

Particles scatter on magnetic field fluctuations.

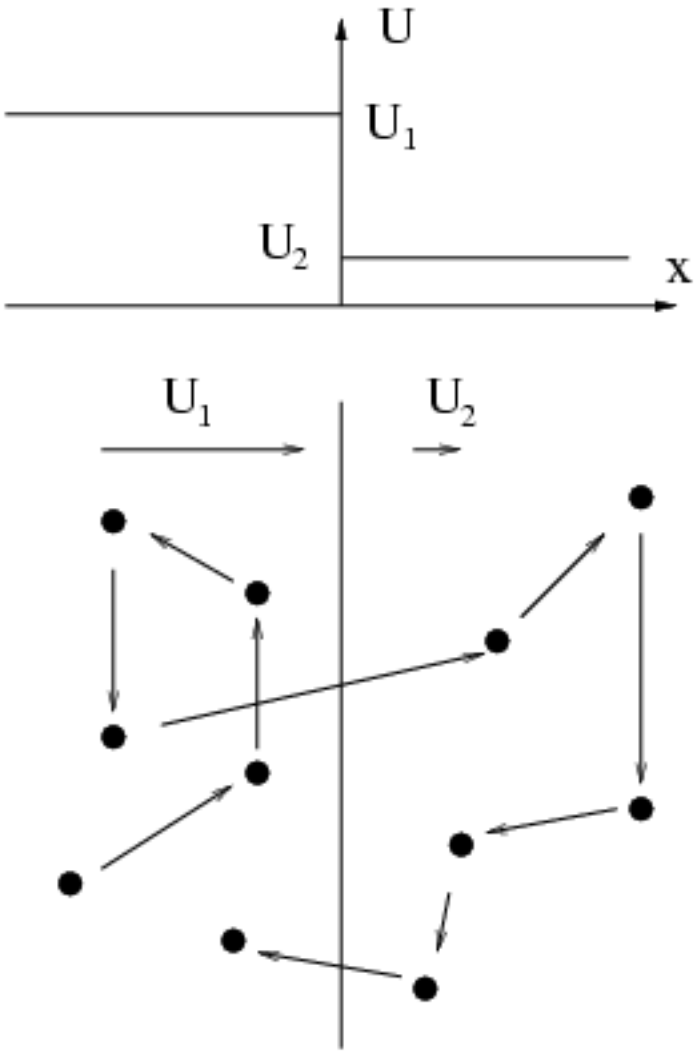

Particles generate magnetic field fluctuations.

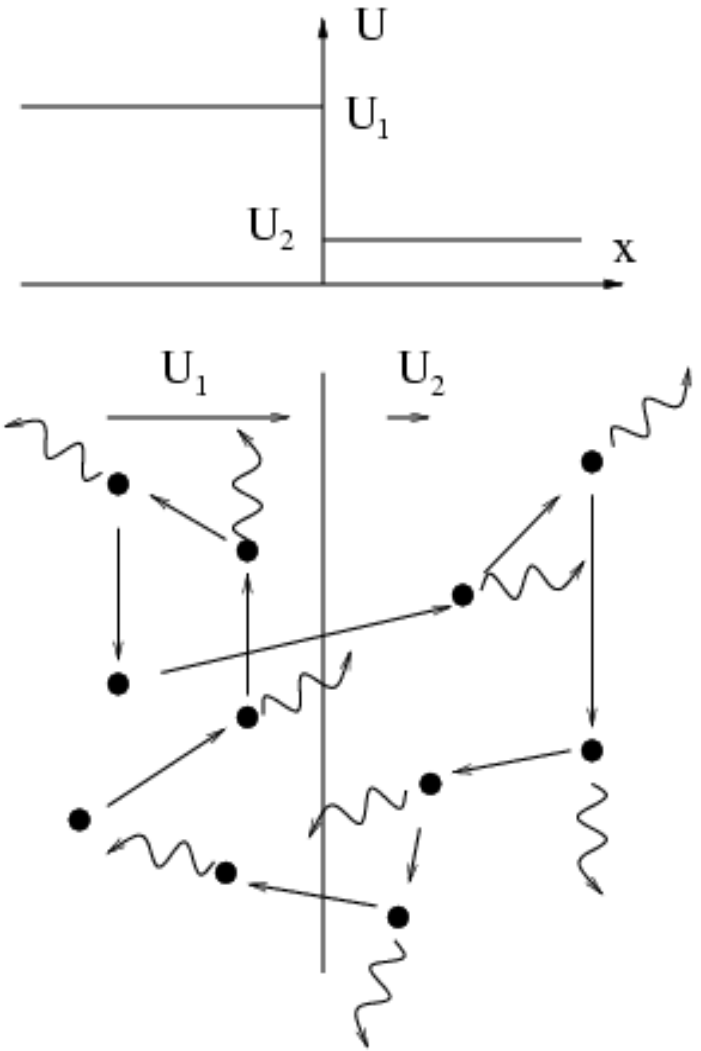

Fermi acceleration at shock - II.

- Particle acceleration and magnetic field generation processes are highly depended on each other. Fermi acceleration is highly nonlinear process.
- Accelerated particles produce additional pressure that can eventually modify hydrodynamic shock velocity profile.
- Test particle approximation is often used in which shock velocity profile and particle diffusion are assumed to be known. In this case particle acceleration process can be described linearly.

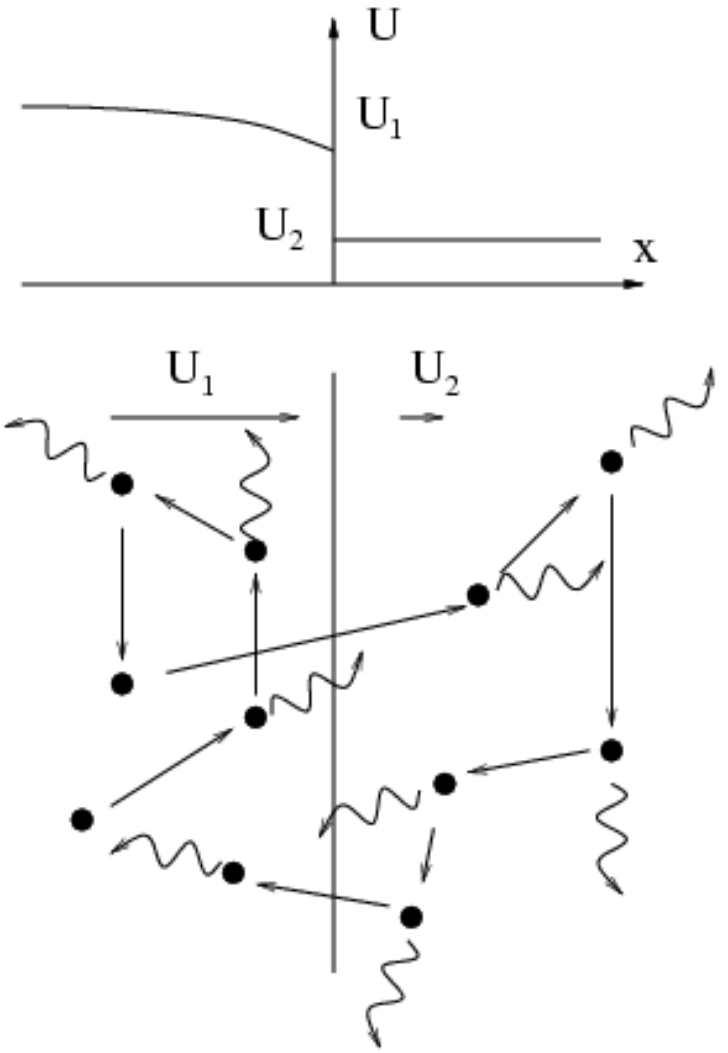

Electron distribution function calculation.

An electron distribution function was calculated according to work *Bykov&Uvarov 1999* with added accounting for synchrotron radiation losses. The diffusion limit of a kinetic equation was used:

$$D(p)\frac{\partial^2 f}{\partial x^2} - u(x)\frac{\partial f}{\partial x} + \frac{p}{3}\frac{\partial f}{\partial p}\frac{\partial u}{\partial x} - \frac{1}{p^2}\frac{\partial}{\partial p}\left(p^2 L(p) f\right) = 0$$

$D(p)=\eta c r_c(p)/3$ is a particle diffusion coefficient (which equals to Bohm diffusion coefficient if $\eta=1$), $r_c(p)=pc/eH$ is a Larmor radius, L(p)=dp/dt is a function of energy losses. On high electron energies we can take into account only synchrotron losses and

$$L(p) = \frac{dp}{dt} = -\frac{32\pi}{9}\left(\frac{e^2}{m_e c^2}\right)^2 \left(\frac{H_{av}^2}{8\pi}\right)\left(\frac{p^2}{m_e^2 c^2}\right)$$

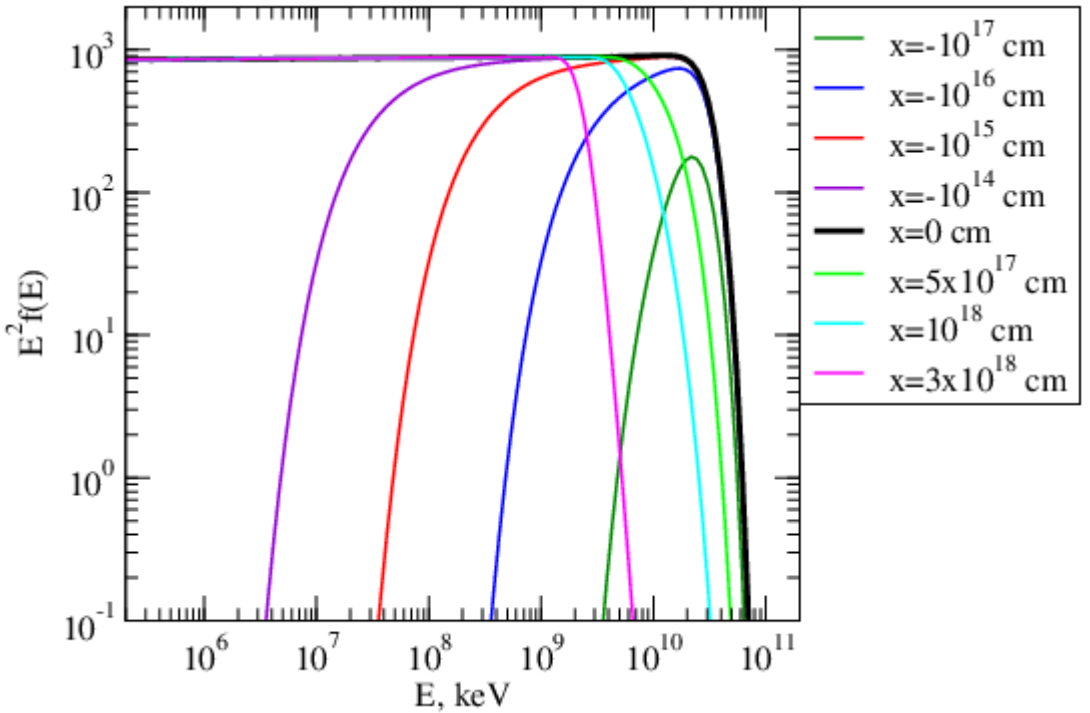

Fig. 1. An electron distribution function in the vicinity of the SNR shock wave is shown for different values of distance from the shock. Negative values correspond to the upstream ($r>R_{SNR}$) region, while positive values correspond to the downstream ($r<R_{SNR}$) region. The magnetic field $H=5\times10^{-5}$ G used in synchrotron losses calculations was taken to be equal to the mean square value of the magnetic field.

Modeling of synchrotron maps.

In order to simulate synchrotron images we need an electron distribution function together with turbulence magnetic field realization.

To obtain SNR synchrotron emission maps we calculated stochastic magnetic field in a box intersecting with SNR shell. We made simulations for isotropic and anisotropic magnetic field turbulence cases. The geometry of the model is shown in the fig. 2. The size and angular size of the model remnant were chosen to match these parameters for Tycho SNR.

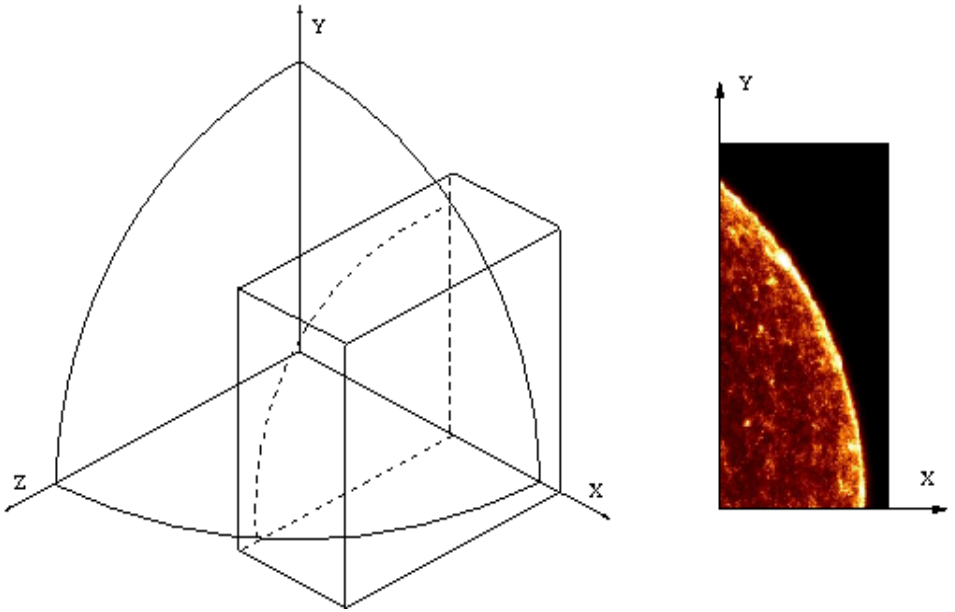

Fig. 2. On the upper left panel the relative position of the SNR remnant and the box where stochastic magnetic field was calculated are shown. The line of sight toward observer is along the Oz axis. On the upper right panel the observed part of the shell is shown with the effect of projection along the line of sight taken into account.

Modeling of an isotropic stochastic magnetic field.

According to our previous works (*Bykov etal 2008, Bykov etal 2009*) we use a method suggested in *Giakalone&Jokipii* 1999. We consider a summation of big number of harmonics with random wave vectors and phases.

$$\mathbf{B}(\mathbf{r},t)=\sum_{n=1}^{N_m}\sum_{\alpha=1}^{2}\mathbf{A}^{(\alpha)}(k_n)\cos\left(\mathbf{k}_n\cdot\mathbf{r}-\omega_n(\mathbf{k}_n)\cdot t+\phi_n^{(\alpha)}\right),$$

Two orthogonal polarizations $\mathbf{A}^{(a)}(k_n)$ (a=1,2) of magnetic field are both orthogonal to the wave vector ($\mathbf{A}^{(a)}(k_n) \perp k_n$) to fulfill zero divergence condition $\nabla \mathbf{B}=0$. We make a summation independent plane waves with randomly distributed wave vectors amplitudes $A^2(k)=C_s<B_s^2>k^{-(\delta+2)}$. This corresponds to a spectral energy density of turbulence magnetic field $W(k)\sim k^{-\delta}\sim k^2A^2(k)$ where δ is an index of power spectrum.

$<B^2>$ is an average square of a magnetic field. The stochastic properties of an isotropic field are $<B_x^2>=<B_y^2>=<B_z^2>=<B^2>/3$.

Modeling of an anisotropic stochastic magnetic field.

We also consider a case of cylindrically symmetric turbulence when an average values have the following properties: $\langle B_{\perp}^2 \rangle = q \langle B_{||}^2 \rangle = q \langle B^2 \rangle / (q+1)$.

The previously described method can be easily extended to this case. Lets consider one particular magnetic harmonic. For the 1st polarization we chose a direction of magnetic field $\mathbf{B}_1$ to lie in a plane made by the symmetry axis and the wave vector (fig. 3). For the 2nd polarization the direction of magnetic field $\mathbf{B}_2$ will be orthogonal both to the symmetry axis and the wave vector. The 2nd polarization gives contribution only to the value of $\mathbf{B}_{\perp}$ while the 1st polarization gives contribution both to $\mathbf{B}_{\perp}$ and $B_{||}$. If we increase an amplitude of the 2nd polarization we get an anisotropic magnetic field with desired properties.

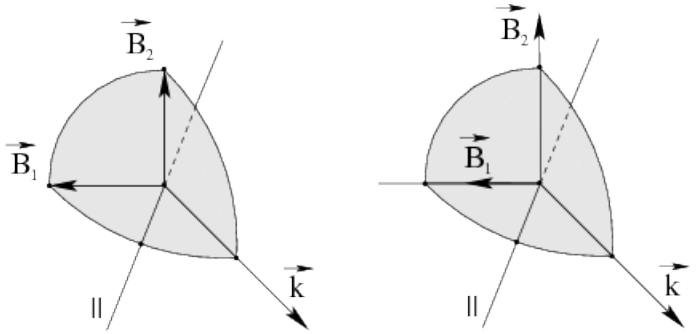

Fig. 3. Direction of the symmetry axis ||, the wave vector and magnetic field polarizations of one particular harmonic are shown. Left and right panels schematically show the isotropic and the anisotropic turbulence cases respectively.

It appears that in the anisotropic case all modeling remains the same as in isotropic case but the amplitudes of harmonics should be slightly different: $A_1^2=(1-a)A^2(k)$, $A_2^2=(1+a)A^2(k)$, $a>0$, $A(k)$ is an amplitude in an isotropic case. It easy to see that parameter $q=(2+a)/(1-a)$.

Anisotropy turbulent magnetic field formation. Compression at a shock front.

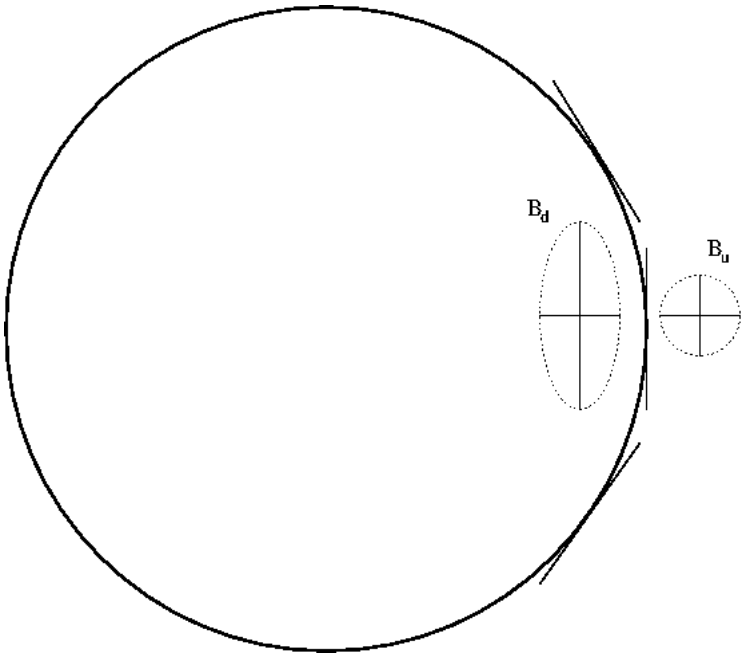

$B_{n,up} = B_{n,down}$

If $B_n = 0$, then $B_{t,up} u_{up} = B_{t,down} u_{down}$

So initially isotropic (in upstream) turbulent magnetic field will be anisotropic in downstream.

Synchrotron emission - I.

Properties of a radiation field can be described by 4 Stokes parameters: I, Q, U, V. These parameters for synchrotron emission of isotropic ultrarelativistic electron distribution with energy spectrum $f_e(E)$ can be represented as *(Ginzburg V.L., Syrovatskii S.I. 1965)*: V=0,

$$I(\nu) = \int I(\nu, \mathbf{r}) dr = \frac{\sqrt{3} e^3}{mc^2} \int dr dE \frac{\nu}{\nu_c} B_\perp (\mathbf{r}) f_e (E, \mathbf{r}) \int\limits_{\nu/\nu_c}^{\infty} K_{5/3}(\eta) d\eta,$$

$$Q(\nu) = \int Q(\nu, \mathbf{r}) dr = \frac{\sqrt{3} e^3}{mc^2} \int dr dE \frac{\nu}{\nu_c} cos\,(2\chi)\, B_\perp (\mathbf{r}) f_e (E, \mathbf{r}) K_{2/3} \left(\frac{\nu}{\nu_c} \right),$$

$$U(\nu) = \int U(\nu, \mathbf{r}) dr = \frac{\sqrt{3} e^3}{mc^2} \int dr dE \frac{\nu}{\nu_c} sin\,(2\chi)\, B_\perp (\mathbf{r}) f_e (E, \mathbf{r}) K_{2/3} \left(\frac{\nu}{\nu_c} \right),$$

$$\nu_c = \frac{3eB_\perp}{4\pi mc} \gamma^2, \int dE d\Omega_E \cdot f_e (E, \mathbf{r}) = 4\pi \int dE \cdot f_e (E, \mathbf{r}) = n(\mathbf{r}).$$

χ is an angle between a chosen direction in a plane perpendicular to wave vector **k** and a major axis of the polarization ellipse. Degree of polarization can be obtained using the formula:

$$\Pi_\nu = \frac{\sqrt{Q_\nu^2 + U_\nu^2 + V_\nu^2}}{I_\nu}$$

Synchrotron emission - II.

The main axis of polarization ellipse of emitting synchrotron radiation is perpendicular locally to the direction of the magnetic field projection $\mathbf{B}_\perp$. If we chose to measure rotation angle of polarization ellipse χ from the **-Ox** axis then $\cos(\chi) = B_{\perp y}/B_\perp$ and $\sin(\chi) = B_{\perp x}/B_\perp$. So we get:

$$Q(\nu) = \frac{\sqrt{3}e^3}{mc^2} \int dr dE \frac{\nu}{\nu_c} B_\perp(\mathbf{r}) f_e(E, \mathbf{r}) K_{2/3}\left(\frac{\nu}{\nu_c}\right) \frac{B_{\perp y}^2 - B_{\perp x}^2}{B_\perp^2}$$

$$U(\nu) = \frac{\sqrt{3}e^3}{mc^2} \int dr dE \frac{\nu}{\nu_c} B_\perp(\mathbf{r}) f_e(E, \mathbf{r}) K_{2/3}\left(\frac{\nu}{\nu_c}\right) \frac{2B_{\perp y} \cdot B_{\perp x}}{B_\perp^2}$$

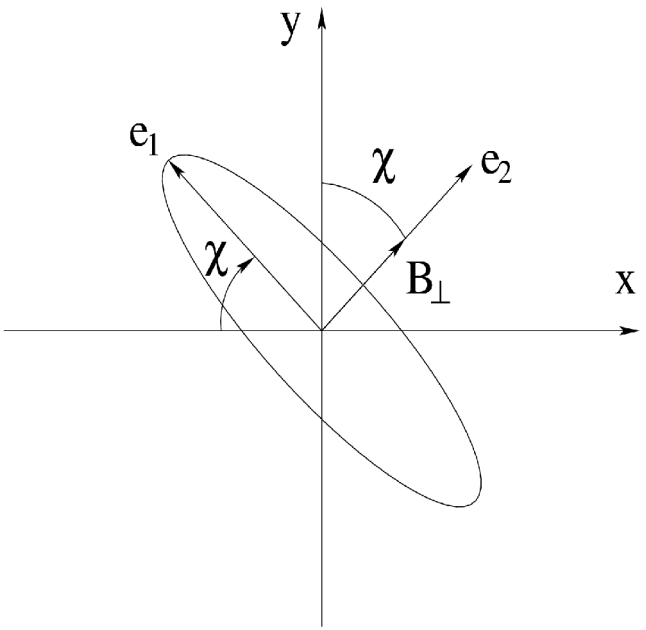

Fig. 4. A polarization ellipse of the emitting radiation and a possible definition of the angle χ is shown. The view is in the direction from the observation point toward the emission region. The transverse to the line of sight part of the magnetic field $\mathbf{B}_\perp$ in the emission region is also shown together with directions of main unit polarization vectors $\mathbf{e}_1$, $\mathbf{e}_2$ directed along main axis of the polarization ellipse.

Synchrotron emission - III.

If we consider an isotropic stochastic magnetic field or an anisotropic field with axial symmetry and the symmetry axis coincides with the direction to the observer then x and y field projections have equal properties and <Q>=0, <U>=0. It means that the average polarization is suppressed and after averaging over an ensemble of all possible stochastic field realizations Q and U should be equal to zero. Practically we see only one particular realization so polarization is not zero but much less then the polarization of synchrotron radiation in a homogeneous magnetic field.

If we consider an anisotropic magnetic field with an axial symmetry and the symmetry axis is perpendicular to the direction toward observer and coincides with axis Ox (or Oy) then x and y field projections have different properties, $<B_{\perp y}^2> \neq <B_{\perp x}^2>$ so $<Q> \neq 0$ while $<U>=0$. If $B_\perp^2/B_\parallel^2$ is high then <Q> can be close to the value for homogeneous magnetic field and polarization can be close to maximum theoretical limit $p=(\gamma+1)/(\gamma+7/3)$ for isotropic power law particle distribution function in homogeneous magnetic field.

$$Q(\nu) = \frac{\sqrt{3}e^3}{mc^2} \int dr dE \frac{\nu}{\nu_c} B_\perp(\mathbf{r}) f_e(E,\mathbf{r}) K_{2/3}\left(\frac{\nu}{\nu_c}\right) \frac{B_{\perp y}^2 - B_{\perp x}^2}{B_\perp^2}$$

$$U(\nu) = \frac{\sqrt{3}e^3}{mc^2} \int dr dE \frac{\nu}{\nu_c} B_\perp(\mathbf{r}) f_e(E,\mathbf{r}) K_{2/3}\left(\frac{\nu}{\nu_c}\right) \frac{2B_{\perp y} \cdot B_{\perp x}}{B_\perp^2}$$

Model synchrotron intensity and polarization maps. Maps for photon energy 5keV, and different anisotropy of the magnetic turbulence, power spectrum index δ=5/3.

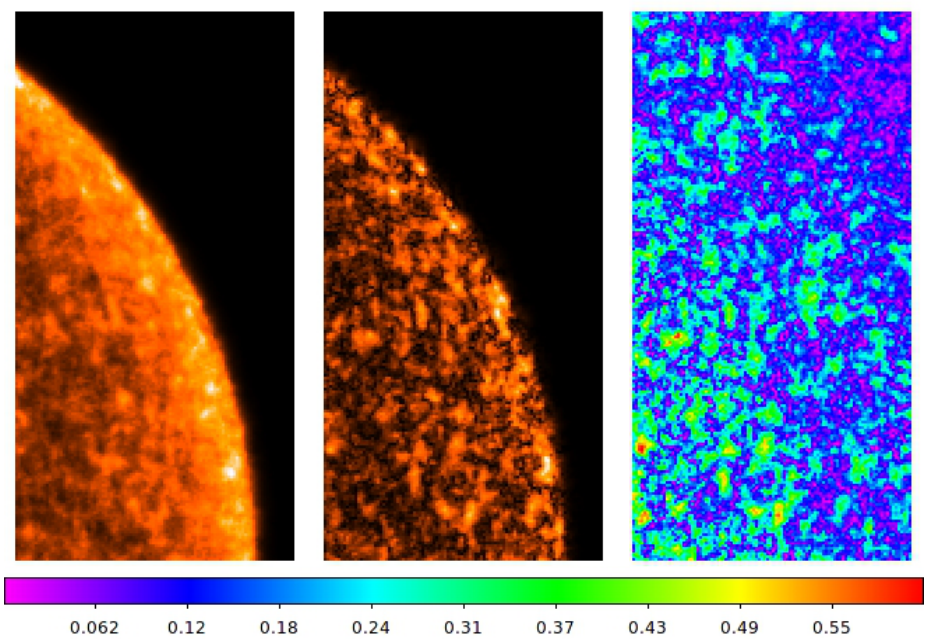

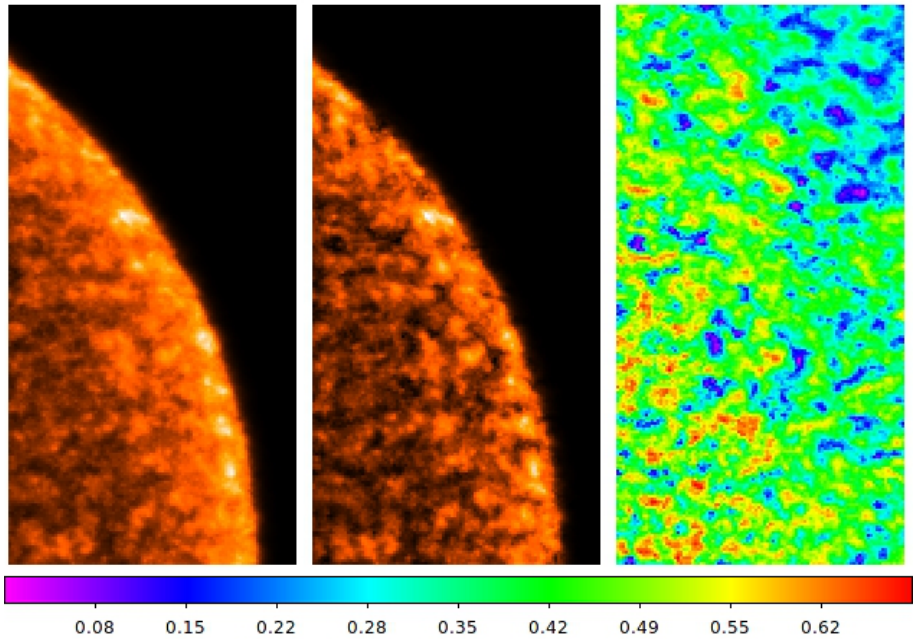

Fig. 5. The model synchrotron images are shown with the angular resolution 1.2". On each panel the total emission is in the left, the polarized emission is in the middle and polarization degree is in the right. The upper left, upper right and lower right panels respectively show an isotropic turbulence case and anisotropic turbulence cases with q=5 and q=20. The value of the power spectrum index of magnetic field fluctuations δ=5/3.

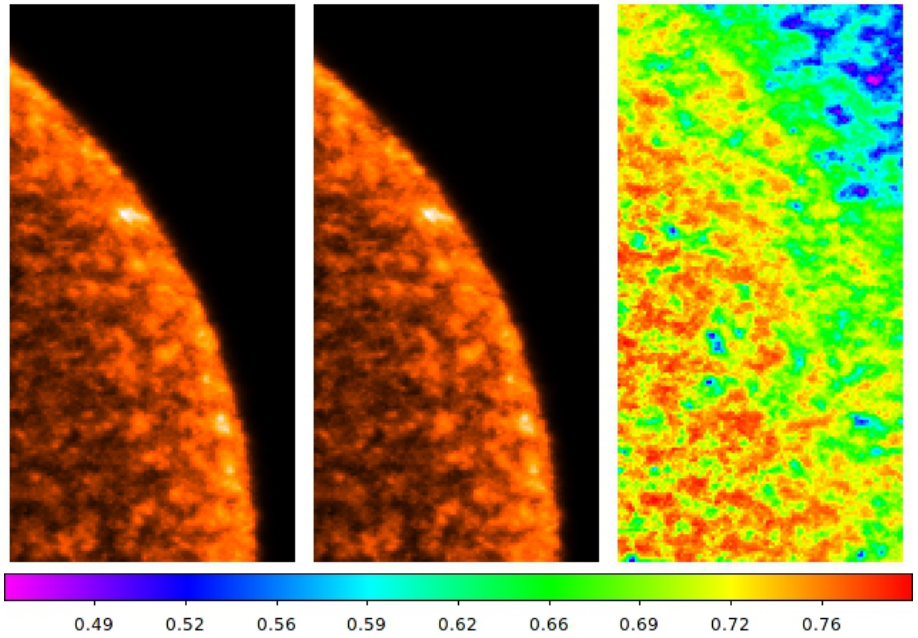

Model synchrotron intensity and polarization maps. Maps for photon energy 5keV and different anisotropy of the magnetic turbulence with power spectrum index δ=1.

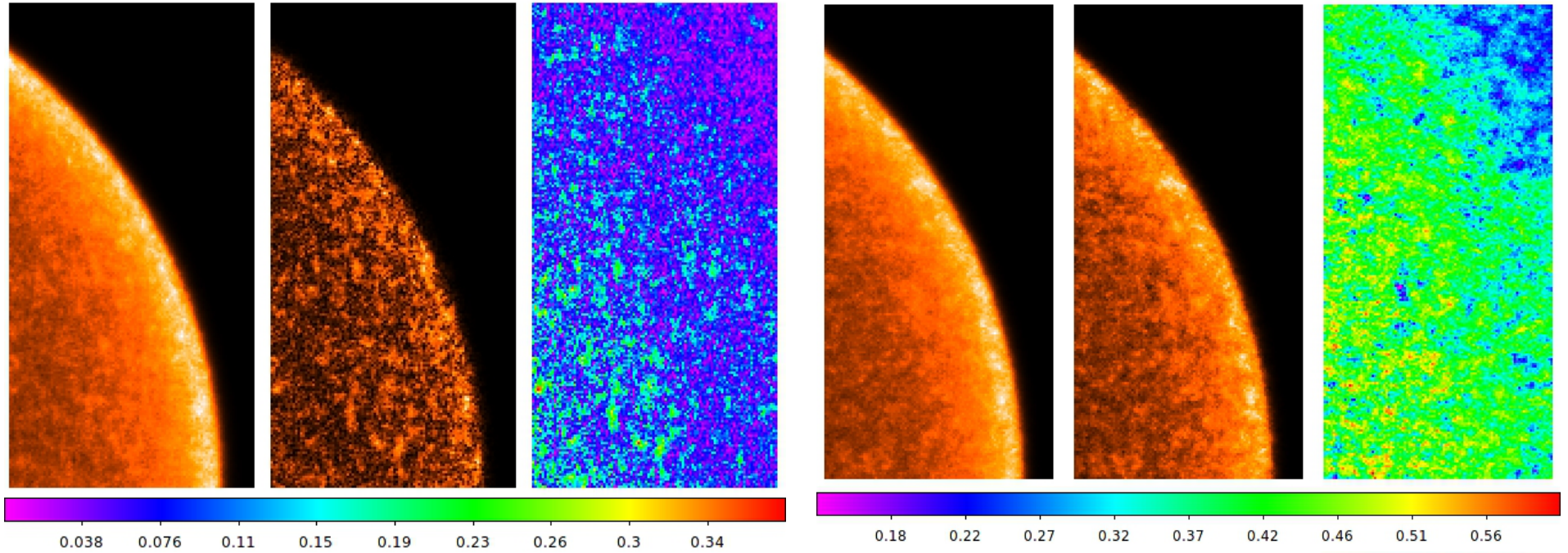

Fig. 6. The model synchrotron images are shown with the angular resolution 1.2". On each panel the total emission is in the left, the polarized emission is in the middle and polarization degree is in the right. The upper left, upper right and lower right panels respectively show an isotropic turbulence case and anisotropic turbulence cases with q=5 and q=20. The value of the power spectrum index of magnetic field fluctuations δ=1.

XIPE

XIPE is a proposed but not yet accepted ESA mission of a new generation X-ray polarimeter. Its detector unit is a Gas Pixel Detector (Costa E. et al. (2001)).

Energy band	2-8 keV
Angular resolution	~ 24 arcsec
Field of view	~ 15x15 arcmin

IXPE

IXPE is a planned NASA mission of a new generation X-ray polarimeter. Its detector unit is a Gas Pixel Detector that has the same design as XIPE detector.

The polarimeter should have almost the same capabilities as XIPE but with slightly lower mirror area.

Maps after convolution with XIPE PSF.
Maps for photon energy 5keV and different anisotropy of the magnetic turbulence with power spectrum index $\delta=5/3$.

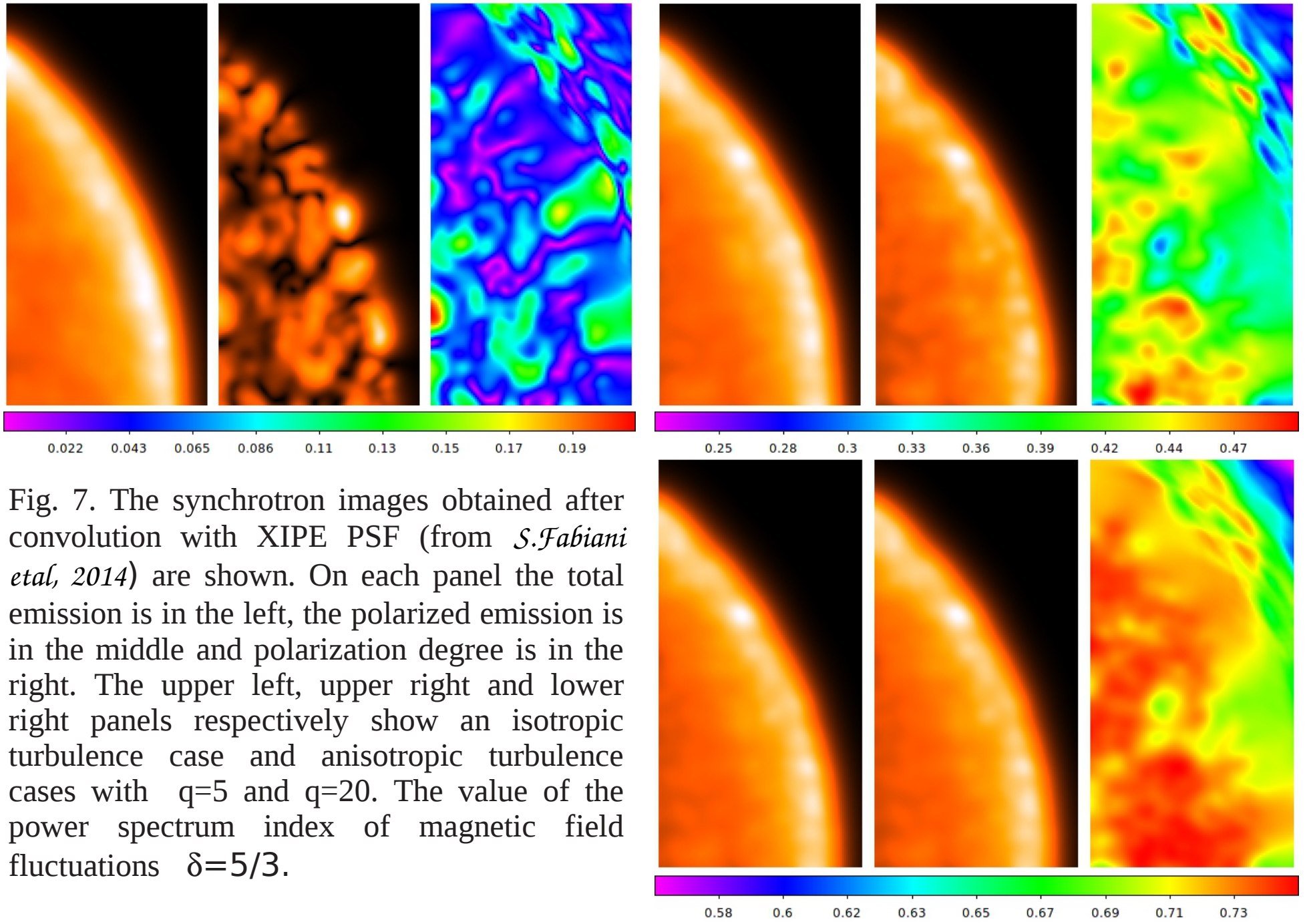

Fig. 7. The synchrotron images obtained after convolution with XIPE PSF (from *S.Fabiani etal, 2014*) are shown. On each panel the total emission is in the left, the polarized emission is in the middle and polarization degree is in the right. The upper left, upper right and lower right panels respectively show an isotropic turbulence case and anisotropic turbulence cases with q=5 and q=20. The value of the power spectrum index of magnetic field fluctuations $\delta=5/3$.

Maps after convolution with XIPE PSF.
Maps for photon energy 5keV and different anisotropy of the magnetic turbulence with power spectrum index δ=1.

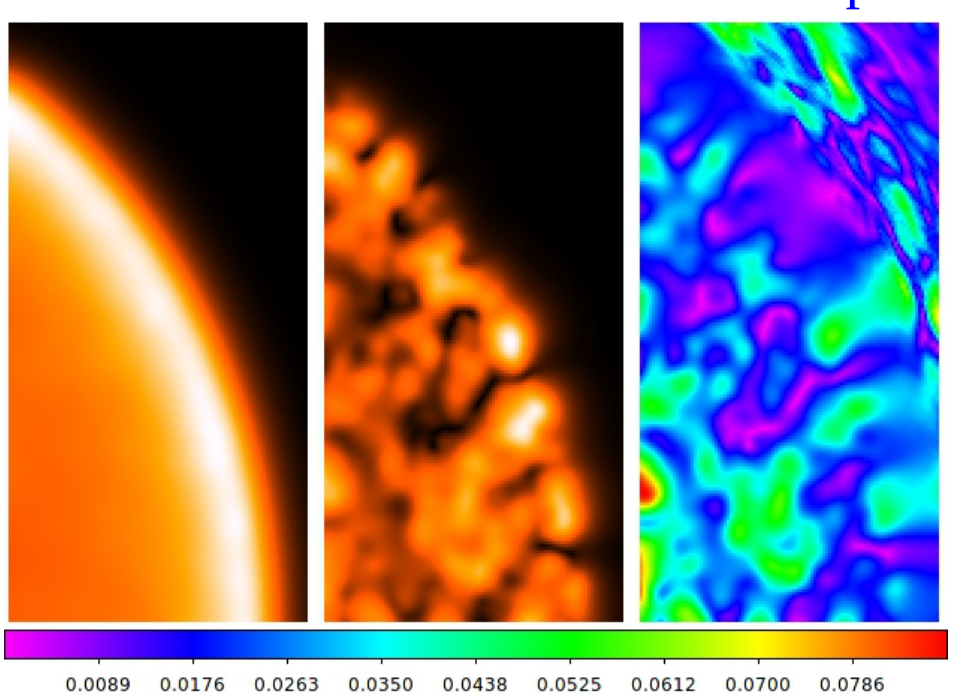

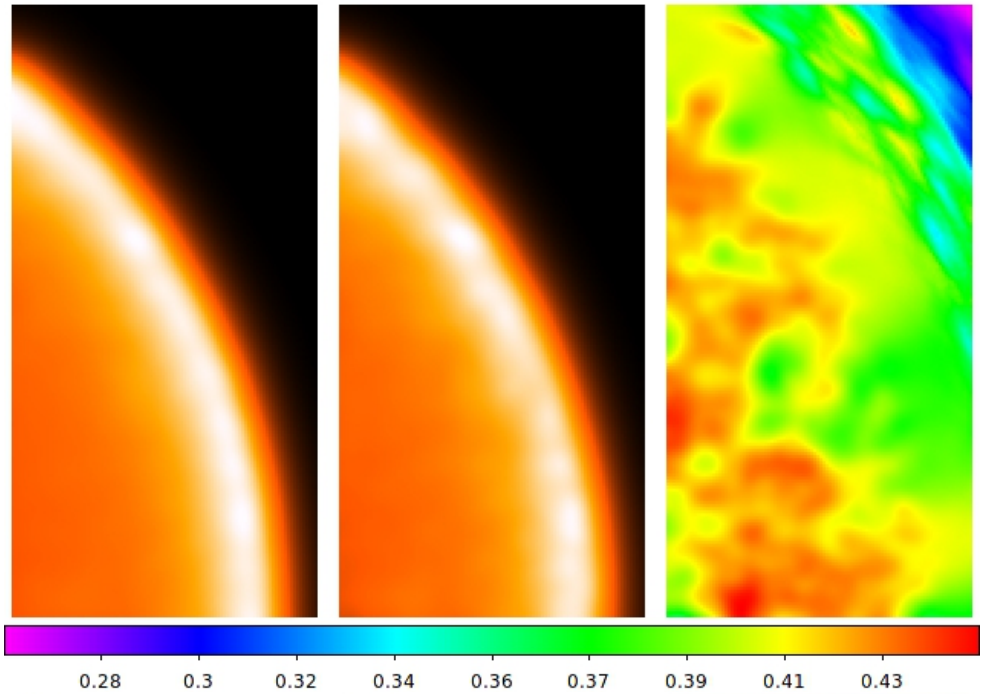

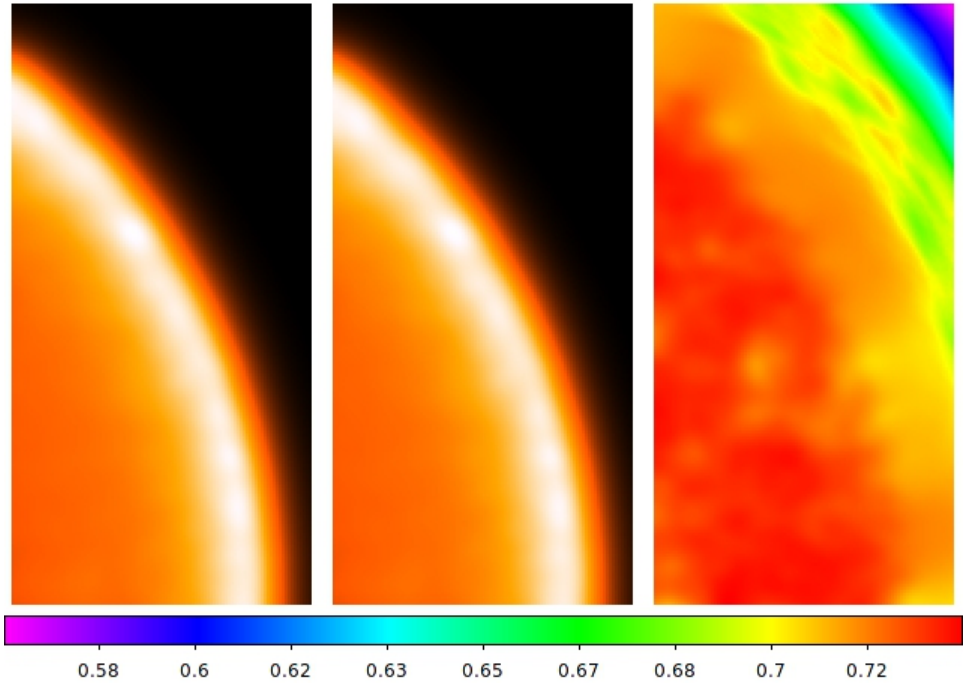

Fig. 8. The synchrotron images obtained after convolution with XIPE PSF (from *S.Fabiani etal, 2014*) are shown. On each panel the total emission is in the left, the polarized emission is in the middle and polarization degree is in the right. The upper left, upper right and lower right panels respectively show an isotropic turbulence case and anisotropic turbulence cases with q=5 and q=20. The value of the power spectrum index of magnetic field fluctuations δ=1.

Bibliography:

- *Bykov A.M., Uvarov Y.A., Ellison D.C., The Astrophysical Journal, v.689 (2008) L133.*
- *Bykov A.M., Uvarov Y.A., JETP, v.88, iss. 3 (1999) pp. 465.*
- *Bykov A.M, Uvarov Y.A., Bloemen J.B.G.M., den Herder J.W., Kaastra J.S., Mon. Not. R. Astron. Soc., v.399, iss. 3 (2009) p. 1119-1125.*
- *Giacalone J., Jokipii J.R., The Astrophysical Journal, v.520 (1999) p. 204-214.*
- *Ginzburg V.L., Syrovatskii S.I., Annual Review of Astronomy and Astrophysics, vol. 3 (1965) p.297.*
- *Fabiani S. etal., The Astrophysical Journal Supplement, v. 212, iss. 2, article id. 25, 13 pp. (2014).*
- *P. Goldreich, S. Sridhar, The Astrophysical Journal, v. 438, 763-775 (1995).*

Acknowledgments:

The authors acknowledge support from RSF grant 16-12-10225. Most calculations were done on computers of the RAS JSCC and St-Petersburg department of RAS JSCC.